Journal of Sound and Vibration (1997) **199**(1), 71–85

FREE VIBRATION ANALYSIS OF SYMMETRICALLY LAMINATED COMPOSITE RECTANGULAR PLATES

J. M. LEE

Hyundai Maritime Research Institute, Ulsan, Korea

AND

J. H. CHUNG AND T. Y. CHUNG

Korea Institute of Machinery and Materials, Daeduk Science Town, Daejeon, Korea

(*Received* 7 *December* 1995, *and in final form* 6 *June* 1996)

Free vibration analysis of symmetrically laminated composite rectangular plates with all edges elastically restrained against rotation was carried out based on the first order anisotropic shear deformation plate theory. The iterative Kantorovich method and the Rayleigh–Ritz method with three different sets of trial functions were applied to the analysis. The numerical results were compared with each other and with experimental ones, and they showed good agreement.

1. INTRODUCTION

The classical thin plate theory gives overestimated results in the free vibration analysis of thick plates, especially for fiber-reinforced laminated composite plates because of their low transverse shear modulus ratio to the in-plane Young's modulus. The effects of shear deformation and rotary inertia should be considered in the governing equations for a reliable prediction of the dynamic behavior of laminated composite plates. Among a number of plate theories including both effects, the first order anisotropic shear deformation theory for laminated composite plates, referred to as the YNS (Yang–Norris–Stavsky) theory [1], is widely adopted for the dynamic analysis of anisotropic laminated composite plates.

Using the YNS theory, Whitney and Pagano [2] and Bert and Chen [3] presented closed form solutions for the free vibration of asymmetric angle-ply plate strips and laminates with all edges simply supported, respectively. For the plates with other boundary conditions, several approximate solutions are common. Craig and Dawe [4] and Chung *et al*. [5] presented the Rayleigh–Ritz solutions by using Timoshenko beam functions and by using Timoshenko beam characteristic polynomials [6] as trial functions, respectively, for the free vibration of symmetrically laminated composite rectangular plates. Bowlus *et al*. [7] presented the Galerkin solutions by using harmonic functions as trial functions. Dawe and Wang [8, 9] presented the spline Rayleigh–Ritz solutions and the spline finite strip solutions for the free vibration of rectangular laminated composite plates.

Recently, Bhat *et al*. [10] and Lee and Kim [11] used the iterative Kantorovich method to obtain plate characteristic functions and natural frequencies of rectangular isotropic

0022–460X/97/010071 + 15 $25.00/0/sv960653

thin plates and thick plates respectively. The results of their numerical examples show that the method gives better accuracy in natural pairs and computational efficiency than other methods.

In this paper, the free vibration analysis of symmetrically laminated composite rectangular plates with all edges elastically restrained against rotation was carried out based on the YNS theory. The iterative Kantorovich method and the Rayleigh–Ritz method were applied to the vibration analysis. Three different sets of trial functions: the newly derived plate characteristic functions, Timoshenko beam functions and characteristic polynomials, were used to obtain the Rayleigh–Ritz solution. Some numerical and experimental applications were performed to verify the usefulness of the presented methods.

2. THE FIRST ORDER ANISOTROPIC SHEAR DEFORMATION PLATE THEORY: THE YNS THEORY

The geometrical configuration and co-ordinate system of a rectangular thick plate is shown in Figure 1 with its boundary conditions, and non-dimensional parameters are introduced as follows:

$$\xi = x/a, \qquad \eta = y/b, \qquad \alpha = a/b,$$

$$K_{Rx_1} = k_{Rx_1}a/D_{11}, \qquad K_{Rx_2} = k_{Rx_2}a/D_{11}, \qquad K_{Ry_1} = k_{Ry_1}b/D_{22}, \qquad K_{Ry_2} = k_{Ry_2}b/D_{22}, \quad (1)$$

where a and b are the plate lengths in the x and y directions respectively, k_R (refer to Figure 1(b) for the additional subscripts x_1, x_2, y_1 and y_2) are the rotational spring

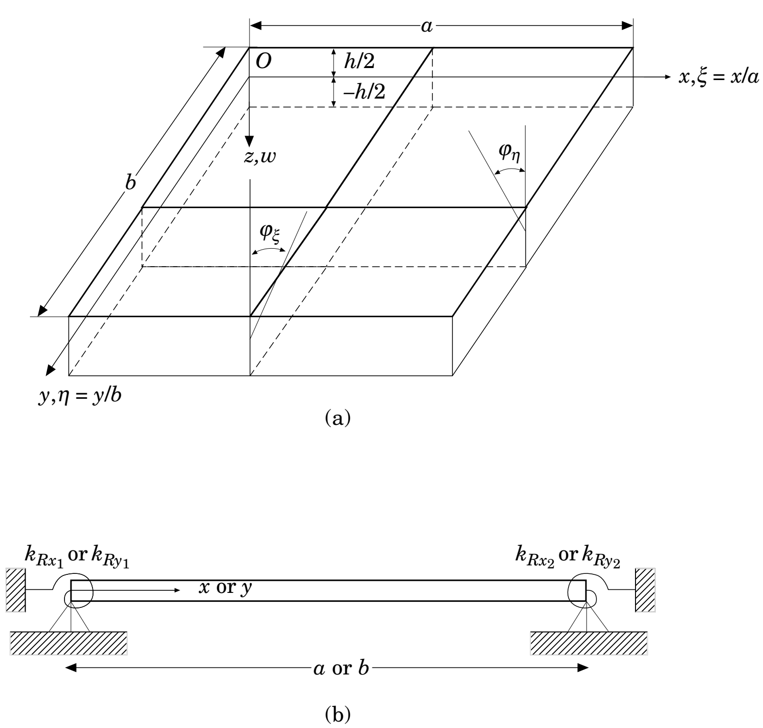

Figure 1. The co-ordinate system (a) and boundary conditions (b) of a rectangular thick plate.

constants, and D_{ii} ($i = 1, 2$) are the flexural rigidities of the plate, to be described in detail later.

Since there is no coupling of extensional/shearing behavior to bending/twisting behavior for the symmetrically laminated composite plate, the YNS theory leads to the following expressions for the strain energy, V, and the kinetic energy, T, of the system:

$$V = \frac{1}{2\alpha}\left[\int_0^1 \int_0^1 \left\{D_{11}\left(\frac{\partial \psi_\xi}{\partial \xi}\right)^2 + \alpha^2 D_{22}\left(\frac{\partial \psi_\eta}{\partial \eta}\right)^2 + 2\alpha D_{12}\frac{\partial \psi_\xi}{\partial \xi}\frac{\partial \psi_\eta}{\partial \eta}\right.\right.$$
$$+ D_{66}\left(\alpha\frac{\partial \psi_\xi}{\partial \eta} + \frac{\partial \psi_\eta}{\partial \xi}\right)^2 + 2D_{16}\frac{\partial \psi_\xi}{\partial \xi}\left(\alpha\frac{\partial \psi_\xi}{\partial \eta} + \frac{\partial \psi_\eta}{\partial \xi}\right)$$
$$+ 2\alpha D_{26}\frac{\partial \psi_\eta}{\partial \eta}\left(\alpha\frac{\partial \psi_\xi}{\partial \eta} + \frac{\partial \psi_\eta}{\partial \xi}\right)$$
$$+ A_{55}\left(\frac{\partial w}{\partial \xi} - a\psi_\xi\right)^2 + \alpha^2 A_{44}\left(\frac{\partial w}{\partial \eta} - b\psi_\eta\right)^2$$
$$\left.+ 2A_{45}\left(a^2\psi_\xi\psi_\eta - a\alpha\psi_\xi\frac{\partial w}{\partial \eta} - a\psi_\eta\frac{\partial w}{\partial \eta} + a\frac{\partial w}{\partial \xi}\frac{\partial w}{\partial \eta}\right)\right\}\mathrm{d}\xi\,\mathrm{d}\eta$$
$$+ D_{11}\int_0^1 (K_{Rx_1}\psi_\xi^2\rfloor_{\xi=0} + K_{Rx_2}\psi_\xi^2\rfloor_{\xi=1})\,\mathrm{d}\eta$$
$$\left.+ \alpha^2 D_{22}\int_0^1 (K_{Ry_1}\psi_\eta^2\rfloor_{\eta=0} + K_{Ry_2}\psi_\eta^2\rfloor_{\eta=1})\,\mathrm{d}\xi\right], \tag{2}$$

$$T = \frac{ab}{2}\int_0^1 \int_0^1 \left\{I\left[\left(\frac{\partial \psi_\xi}{\partial t}\right)^2 + \left(\frac{\partial \psi_\eta}{\partial t}\right)^2\right] + \bar{m}\left(\frac{\partial w}{\partial t}\right)^2\right\}\mathrm{d}\xi\,\mathrm{d}\eta, \tag{3}$$

where $w(\xi, \eta, t)$ is the displacement in the z direction, and $\psi_\xi(\xi, \eta, t)$ and $\psi_\eta(\xi, \eta, t)$ are the cross-sectional rotations in the ξ- and η-directions respectively, as shown in Figure 1.

For the symmetrically laminated composite rectangular plate with thickness h shown in Figure 2, the flexural rigidities D_{ij} ($i, j = 1, 2, 6$) and the shear rigidities A_{ij} ($i, j = 4, 5$) in equation (2) are estimated as follows (see, for example, reference [12]):

$$D_{ij} = \int_{-h/2}^{h/2} \overline{Q_{ij}} z^2\,\mathrm{d}z$$
$$= \tfrac{2}{3}\left[\sum_{m=1}^{N-1} (\overline{Q_{ij}})_m (h_m^3 - h_{m+1}^3) + (\overline{Q_{ij}})_N h_N^3\right] \qquad \text{for } i, j = 1, 2, 6, \tag{4}$$

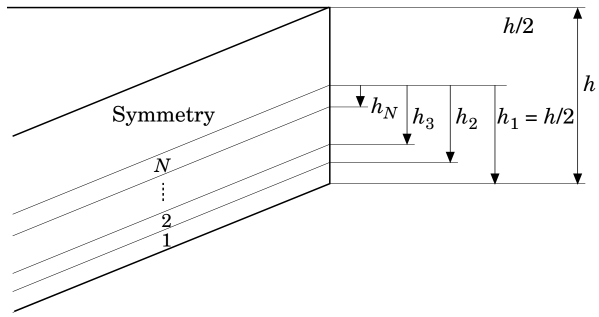

Figure 2. The laminate nomenclature for symmetrically laminated composite plates.

$$A_{ij} = k_i k_j \int_{-h/2}^{h/2} \overline{C_{ij}}\, \mathrm{d}z$$

$$= 2k_i k_j \left[\sum_{m=1}^{N-1} (\overline{C_{ij}})_m (h_m - h_{m+1}) + (\overline{C_{ij}})_N h_N \right]$$

$$= k_i k_j S_{ij} \qquad \text{for } i, j = 4, 5, \tag{5}$$

where $(\overline{Q_{ij}})_m$ and $(\overline{C_{ij}})_m$ are the plane-stress reduced stiffness coefficients and the shear stiffness coefficients of the mth layer with respect to the plate co-ordinates respectively, h_m is the distance from the median surface of the plate to the lower surface of the mth layer and N denotes the number of layers in the half-thickness of the plate. These coefficients may vary from layer to layer depending on the material properties and the lamina orientation of each layer.

The shear correction factors $k_i k_j$ are introduced to allow for the fact that the transverse shear strain distributions are not uniform through the plate thickness. An appropriate estimation of these factors is very important in the YNS theory, but studies on this matter are relatively scarce. Chow [13] derived formulae for the shear correction factors of orthotropic plates with symmetric lamination considering static cylindrical bending, and Whitney [14] extended this to cases of non-symmetric laminates. In this paper, the explicit formulae for the shear correction factors of symmetrically laminated composite plates based on Chow's study are given as follows:

$$\frac{1}{k_i^2} = 2S_{ii} \left[\sum_{m=1}^{N} \frac{1}{(\overline{C_{ii}})_m} \left\{ a_m^2 (h_m - h_{m+1}) - \frac{a_m (\overline{Q_{jj}})_m}{3D_{jj}} (h_m^3 - h_{m+1}^3) + \frac{1}{20} \frac{(\overline{Q_{jj}^2})_m}{D_{jj}^2} (h_m^5 - h_{m+1}^5) \right\} \right], \qquad i = 4, 5; \quad j = 6 - i, \tag{6}$$

where $a_1 = h_1^2 (\overline{Q_{jj}})_1 / 2D_{jj}$, $a_m = a_{m-1} + (h_m^2 / 2D_{jj}) \{ (\overline{Q_{jj}})_m - (\overline{Q_{jj}})_{m-1} \}$ and $h_{N+1} = 0$.

The mass $\bar{m}$ and rotary inertia I per unit area of the plate in equation (3) are evaluated as follows:

$$\bar{m} = \int_{-h/2}^{h/2} \rho \, \mathrm{d}z$$

$$= 2 \left[\sum_{m=1}^{N-1} \rho_m (h_m - h_{m+1}) + \rho_N h_N \right]$$

$$I = \int_{-h/2}^{h/2} \rho z^2 \, \mathrm{d}z$$

$$= \tfrac{2}{3}\left[\sum_{m=1}^{N-1} \rho_m (h_m^3 - h_{m+1}^3) + \rho_N h_N^3\right], \tag{7}$$

where ρ_m is the mass density of the mth layer.

3. THE ITERATIVE KANTOROVICH METHOD AND DERIVATION OF PLATE CHARACTERISTIC FUNCTIONS

In this section, the iterative Kantorovich method [8, 9] is presented to obtain plate characteristic functions and natural pairs of the symmetrically laminated composite rectangular plate with all edges elastically restrained against rotation by iterative reduction of the plate partial differential equation to an ordinary differential equation and solving it exactly. This procedure itself is similar to that used in reference [9].

Assuming the harmonic motion

$$w(\xi, \eta, t) = W(\xi, \eta)\, \mathrm{e}^{\mathrm{i}\omega t}, \qquad \psi_\xi(\xi, \eta, t) = \Psi_\xi(\xi, \eta)\, \mathrm{e}^{\mathrm{i}\omega t},$$
$$\psi_\eta(\xi, \eta, t) = \Psi_\eta(\xi, \eta)\, \mathrm{e}^{\mathrm{i}\omega t} \tag{8}$$

and that the variations of Ψ_ξ and W (Ψ_η and W) in the η direction (ξ direction) are quite similar to each other [15], separation of the spatial variables can be undertaken as follows:

$$W(\xi, \eta) = X(\xi) Y(\eta), \qquad \Psi_\xi(\xi, \eta) = \Phi(\xi) Y(\eta), \qquad \Psi_\eta(\xi, \eta) = X(\xi)\Theta(\eta). \tag{9}$$

By virtue of expressions (9), the variations of W, Ψ_ξ and Ψ_η in the application of Hamilton's principle,

$$\delta \int_{t_1}^{t_2} (T - V)\, \mathrm{d}t = 0,$$

can be expressed as follows:

$$\delta W = \delta X Y + X \delta Y, \qquad \delta \Psi_\xi = \delta \Phi Y + \delta Y \Phi, \qquad \delta \Psi_\eta = \delta X \Theta + \delta \Theta X. \tag{10}$$

At the start of the application of the Kantorovich method, Timoshenko beam functions consistent with the boundary conditions of the plate are adopted as an assumption of deflection shapes along one direction; say, the η direction—$Y(\eta)$ and $\Theta(\eta)$. Timoshenko beam functions with ends elastically restrained against rotation were derived in reference [6].

Since $Y(\eta)$ and $\Theta(\eta)$ are assumed *a priori*, one can take $\delta Y = 0 = \delta \Theta$ in the mathematical operation of the application of Hamilton's principle, which leads the boundary value problem with respect to $X(\xi)$ and $\Phi(\xi)$ as follows:

governing equations,

$$\frac{\mathrm{d}^2\Phi}{\mathrm{d}\xi^2} + \beta_{11}\frac{\mathrm{d}\Phi}{\mathrm{d}\xi} + \beta_{12}\Phi + \frac{\gamma_{11}}{a}\frac{\mathrm{d}^2X}{\mathrm{d}\xi^2} + \frac{\gamma_{12}}{a}\frac{\mathrm{d}X}{\mathrm{d}\xi} + \frac{\gamma_{13}}{a}X = 0,$$

$$\frac{1}{a}\frac{\mathrm{d}^2X}{\mathrm{d}\xi^2} + \frac{\beta_{21}}{a}\frac{\mathrm{d}X}{\mathrm{d}\xi} + \frac{\beta_{22}}{a}X + \gamma_{21}\frac{\mathrm{d}^2\Phi}{\mathrm{d}\xi^2} + \gamma_{22}\frac{\mathrm{d}\Phi}{\mathrm{d}\xi} + \gamma_{23}\Phi = 0; \tag{11}$$

boundary conditions,

$$\frac{\mathrm{d}\Phi}{\mathrm{d}\xi} + \left(\alpha\frac{D_{16}}{D_{11}}A_3 - K_{Rx_1}\right)\Phi + \alpha\frac{D_{16}}{D_{11}}\frac{A_4}{a}\frac{\mathrm{d}X}{\mathrm{d}\xi} + \alpha^2\frac{D_{12}}{D_{11}}\frac{A_2}{a}X = 0,$$

$$\frac{1}{a}\frac{\mathrm{d}X}{\mathrm{d}\xi} + \left(\alpha\frac{D_{26}}{D_{66}}B_7 - ab\frac{A_{45}}{D_{66}}(B_9 - B_8)\right)\frac{1}{a}X$$

$$+\frac{1}{\alpha}\frac{D_{16}}{D_{66}}B_9\frac{\mathrm{d}\Phi}{\mathrm{d}\xi} + \left(B_4 - \frac{b^2A_{55}}{D_{66}}B_2\right)\Phi = 0 \qquad \text{along } \xi = 0, \tag{12}$$

$$\frac{\mathrm{d}\Phi}{\mathrm{d}\xi} + \left(\alpha\frac{D_{16}}{D_{11}}A_3 + K_{Rx_1}\right)\Phi + \alpha\frac{D_{16}}{D_{11}}\frac{A_4}{a}\frac{\mathrm{d}X}{\mathrm{d}\xi} + \alpha^2\frac{D_{12}}{D_{11}}\frac{A_2}{a}X = 0,$$

$$\frac{1}{a}\frac{\mathrm{d}X}{\mathrm{d}\xi} + \left(\alpha\frac{D_{26}}{D_{66}}B_7 - ab\frac{A_{45}}{D_{66}}(B_9 - B_8)\right)\frac{1}{a}X$$

$$+\frac{1}{\alpha}\frac{D_{16}}{D_{66}}B_9\frac{\mathrm{d}\Phi}{\mathrm{d}\xi} + \left(B_4 - \frac{b^2A_{55}}{D_{66}}B_2\right)\Phi = 0 \qquad \text{along } \xi = 1. \tag{13}$$

Here

$$\beta_{11} = \alpha\frac{D_{16}}{D_{11}}(2A_3 - G_{31} + G_{30}), \qquad \beta_{12} = \Omega^2 - a^2\frac{A_{55}}{D_{11}} + \alpha^2\frac{D_{66}}{D_{11}}(A_1 - G_{11} + G_{10}),$$

$$\gamma_{11} = \alpha\frac{D_{16}}{D_{11}}A_4, \qquad \gamma_{12} = \alpha^2\left[\frac{D_{12}}{D_{11}}A_2 + b^2\frac{A_{55}}{D_{11}} + \frac{D_{66}}{D_{11}}(A_2 - G_{21} + G_{20})\right],$$

$$\gamma_{13} = \alpha^3\frac{D_{26}}{D_{11}}(A_5 - G_{41} + G_{40}) + \alpha^2 ab\frac{A_{45}}{D_{11}}(A_3 - A_4),$$

$$\beta_{21} = \alpha\left[\frac{D_{26}}{D_{66}}(2B_7 - S_1 + S_0) + \frac{b^2A_{45}}{D_{66}}(2B_8 - T_1 + T_{10})\right],$$

$$\beta_{22} = \Omega^2\frac{D_{11}}{D_{66}}\left(B_1 + \frac{b^2\bar{m}}{I}B_2\right) + \alpha^2\frac{D_{22}}{D_{66}}(B_3 - H_{11} + H_{10} - K_{Ry_1}S_0 - K_{Ry_2}S_1)$$

$$+\frac{a^2A_{44}}{D_{66}}(B_4 - B_1 + B_5 - B_6 - H_{21} + H_{20} + H_{31} - H_{30}),$$

$$\gamma_{21} = \frac{1}{a}\frac{D_{16}}{D_{66}}B_9, \qquad \gamma_{22} = \frac{D_{12}}{D_{66}}(B_4 - H_{31} + H_{30}) + B_4 - \frac{b^2A_{55}}{D_{66}}B_2,$$

$$\gamma_{23} = \alpha\frac{D_{26}}{D_{66}}(B_{10} - H_{41} + H_{40}) - ab\frac{A_{45}}{D_{66}}(B_9 + B_8 - T_1 + T_0). \tag{14}$$

In equation (14), Ω^2 is the frequency parameter, defined as

$$\Omega^2 = a^2I\omega^2/D_{11} \tag{15}$$

and the other constants given in capital letters in equations (12), (13) and (14) can be evaluated with the functions $Y(\eta)$ and $\Theta(\eta)$ assumed *a priori* as follows:

$$A = \frac{1}{b^2}\int_0^1 Y^2\,\mathrm{d}\eta, \qquad B = \int_0^1 \Theta^2\,\mathrm{d}\eta + \frac{b^2 A_{55}}{D_{66}} A, \qquad A_1 = \frac{1}{A}\frac{1}{b^2}\int_0^1 Y\frac{\mathrm{d}^2 Y}{\mathrm{d}\eta^2}\,\mathrm{d}\eta,$$

$$A_2 = \frac{1}{A}\frac{1}{b}\int_0^1 Y\frac{\mathrm{d}\Theta}{\mathrm{d}\eta}\,\mathrm{d}\eta, \qquad A_3 = \frac{1}{A}\frac{1}{b^2}\int_0^1 Y\frac{\mathrm{d}Y}{\mathrm{d}\eta}\,\mathrm{d}\eta, \qquad A_4 = \frac{1}{A}\frac{1}{b}\int_0^1 Y\Theta\,\mathrm{d}\eta,$$

$$A_5 = \frac{1}{A}\frac{1}{b}\int_0^1 Y\frac{\mathrm{d}^2\Theta}{\mathrm{d}\eta^2}\,\mathrm{d}\eta, \qquad B_1 = \frac{1}{B}\int_0^1 \Theta^2\,\mathrm{d}\eta, \qquad B_2 = \frac{A}{B},$$

$$B_3 = \frac{1}{B}\int_0^1 \Theta\frac{\mathrm{d}^2\Theta}{\mathrm{d}\eta^2}\,\mathrm{d}\eta, \qquad B_4 = \frac{1}{B}\frac{1}{b}\int_0^1 \frac{\mathrm{d}Y}{\mathrm{d}\eta}\Theta\,\mathrm{d}\eta, \qquad B_5 = \frac{1}{B}\frac{1}{b^2}\int_0^1 Y\frac{\mathrm{d}^2 Y}{\mathrm{d}\eta^2}\,\mathrm{d}\eta,$$

$$B_6 = \frac{1}{B}\frac{1}{b}\int_0^1 Y\frac{\mathrm{d}\Theta}{\mathrm{d}\eta}\,\mathrm{d}\eta, \qquad B_7 = \frac{1}{B}\int_0^1 \Theta\frac{\mathrm{d}\Theta}{\mathrm{d}\eta}\,\mathrm{d}\eta, \qquad B_8 = \frac{A}{B}A_3, \qquad B_9 = \frac{A}{B}A_4,$$

$$B_{10} = \frac{1}{B}\frac{1}{b}\int_0^1 \frac{\mathrm{d}^2 Y}{\mathrm{d}\eta^2}\Theta\,\mathrm{d}\eta, \qquad G_{10}, G_{11} = \frac{1}{A}\frac{1}{b^2}\left[Y\frac{\mathrm{d}Y}{\mathrm{d}\eta}\right]_{\eta=0,1}, \qquad G_{20}, G_{21} = \frac{1}{A}\frac{1}{b}[Y\Theta]_{\eta=0,1},$$

$$G_{30}, G_{31} = \frac{1}{A}\frac{1}{b^2}[Y|_{\eta=0,1}]^2, \qquad G_{40}, G_{41} = \frac{1}{A}\frac{1}{b}\left[Y\frac{\mathrm{d}\Theta}{\mathrm{d}\eta}\right]_{\eta=0,1},$$

$$H_{10}, H_{11} = \frac{1}{B}\left[\Theta\frac{\mathrm{d}\Theta}{\mathrm{d}\eta}\right]_{\eta=0,1},$$

$$H_{20}, H_{21} = \frac{A}{B}G_{10,11}, \qquad H_{30}, H_{31} = \frac{A}{B}G_{20,21}, \qquad H_{40}, H_{41} = \frac{1}{B}\frac{1}{b}\left[\frac{\mathrm{d}Y}{\mathrm{d}\eta}\Theta\right]_{\eta=0,1},$$

$$S_0, S_1 = \frac{1}{B}[\Theta|_{\eta=0,1}]^2, \qquad T_0, T_1 = \frac{1}{B}\frac{1}{b^2}[Y|_{\eta=0,1}]^2. \tag{16}$$

From the general solution of equations (11) and the boundary conditions (12) and (13), an eigenvalue problem can be obtained, the solution of which gives the frequency parameter Ω_{ij} and the corresponding functions $X(\xi)$ and $\Phi(\xi)$. This procedure is described in detail in the Appendix.

By using $X(\xi)$ and $\Phi(\xi)$ obtained in the previous step as the deflection shapes along the ξ direction, and through a similar mathematical operation, the frequency parameter $\Omega_{ij}^* = \sqrt{a^2 I\omega^2/D_{11}}$ and the corresponding functions $Y(\eta)$ and $\Theta(\eta)$ in the η direction can be obtained by the same way as Ω_{ij}, $X(\xi)$ in the ξ direction.

This iteration process is continued until the condition $|\Omega_{ij} - \Omega_{ij}^*| < \varepsilon$ is satisfied, where ε is the prescribed relative error convergence criterion.

Consequently, the plate characteristic functions consisting of the above resulting functions in both the ξ and the η directions are obtainable in accordance with equations (9).

4. THE RAYLEIGH–RITZ ANALYSIS

In the Rayleigh–Ritz analysis, trial functions for $W(\xi, \eta)$, $\Psi_\xi(\xi, \eta)$ and $\Psi_\eta(\xi, \eta)$ in equations (8) are assumed as follows [4, 5]:

$$W(\xi, \eta) = \sum_{m=1}^{p} \sum_{n=1}^{q} A_{mn} X_m(\xi) Y_n(\eta),$$

$$\Psi_\xi(\xi, \eta) = \sum_{m=1}^{p} \sum_{n=1}^{q} B_{mn} \Phi_m(\xi) Y_n(\eta), \qquad \Psi_\eta(\xi, \eta) = \sum_{m=1}^{p} \sum_{n=1}^{q} C_{mn} X_m(\xi) \Theta_n(\eta) \tag{17}$$

In this paper, three different sets of trial functions $X_m(\xi)$ and $\Phi_m(\xi)$ in the ξ direction (and $Y_n(\eta)$ and $\Theta_n(\eta)$ in the η direction) in equations (18) are considered: the newly derived plate characteristic functions, Timoshenko beam functions and characteristic polynomials, all of which are consistent with the boundary conditions of the plate. For a uniform Timoshenko beam with ends elastically restrained against rotation, the corresponding beam functions and polynomials were derived in reference [6].

The Rayleigh quotient is defined by

$$R(W, \Psi_\xi, \Psi_\eta) = V_{max}/T^*, \tag{18}$$

where V_{max} and T^* are the maximum strain energy and the reference kinetic energy of the system respectively, which can be easily obtained by introducing the expressions of harmonic motion (8) into the energy expressions of the system (2) and (3).

The Rayleigh quotient, R, has the minimum value of Λ when the following conditions are satisfied:

$$\frac{\partial V_{max}}{\partial A_{ij}} - \Lambda \frac{\partial T^*}{\partial A_{ij}} = 0, \qquad \frac{\partial V_{max}}{\partial B_{ij}} - \Lambda \frac{\partial T^*}{\partial B_{ij}} = 0, \qquad \frac{\partial V_{max}}{\partial C_{ij}} - \Lambda \frac{\partial T^*}{\partial C_{ij}} = 0. \tag{19}$$

Equations (19) lead to the eigenvalue problem of matrix form, the solution of which gives the approximate natural frequencies and mode shapes of the system.

5. NUMERICAL AND EXPERIMENTAL APPLICATIONS AND DISCUSSION

For the verification of the validity of the presented methods for free vibration analysis of symmetrically laminated composite rectangular plates, some numerical and experimental investigations were carried out.

5.1. NUMERICAL APPLICATIONS

Two square plate models are taken as numerical examples. The first plate model is a five-layer orthotropic cross-ply laminate (0°/90°/0°/90°/0°) of side length a, with thickness ratio $h/a = 0{\cdot}1$. The material properties for all of the plies are identical and correspond to a typical high modulus fiber composite with $E_1/E_2 = 30$, $G_{12}/E_2 = G_{13}/E_2 = 0{\cdot}6$, $G_{23}/E_2 = 0{\cdot}5$ and $\nu_{12} = 0{\cdot}25$, where the subscripts 1, 2 and 3 denote the directions parallel to the fibers, transverse to the fibers and parallel to the plate thickness respectively. The thickness of the 0° ply is two-thirds of that of the 90° ply. The shear correction factors calculated by equation (6) are $k_4^2 = 0{\cdot}59139$ and $k_5^2 = 0{\cdot}87323$.

The second plate model is the single layer plate of orthotropic material, but the principal material axes are oriented at an angle of 30° to the geometric axis of the plate. The ratio of thickness to side length is $h/a = 0{\cdot}1$ and material properties are $E_1/E_2 = 10$,

$G_{12}/E_2 = G_{23}/E_2 = G_{13}/E_2 = 0{\cdot}25$ and $\nu_{12} = 0{\cdot}3$. The shear correction factors calculated by equation (6) are $k_4^2 = k_5^2 = 5/6$.

In Table 1 are shown the calculated natural frequency parameters $\Omega = \omega\sqrt{\rho a^2/E_2}$ of the first plate model by the iterative Kantorovich method. Two kinds of boundary conditions are considered for the comparisons of the available Rayleigh–Ritz solutions: all edges simply supported (SSSS), i.e., $K_R = 0$, and clamped (CCCC), $K_R = \infty$. In the iteration the relative error convergence criterion is 1×10^{-6}. As shown in Table 1, the results of the iterative Kantorovich method after the second iteration are in good agreement with the Rayleigh–Ritz solutions obtained by using Timoshenko beam functions [4] and by using characteristic polynomials [5].

In general, nodal line patterns of anisotropic angle-ply laminates such as those of the second plate model are skew with respect to the plate co-ordinates, while those of orthotropic cross-ply laminates such as those of the first plate model are usually parallel to the plate co-ordinates (see Figure 3). Since the nodal lines of the plate in the application of the iterative Kantorovich method should be parallel to the plate co-ordinates, it is impractical to apply the iterative Kantorovich method to the vibration analysis of anisotropic angle-ply laminates directly. In these cases, the Rayleigh–Ritz method using the derived plate characteristic functions is applicable to the analysis instead of the iterative Kantorovich method.

For the second plate model with all edges clamped, the Rayleigh–Ritz solutions of the frequency parameter $\Omega = \omega\sqrt{\rho a^2/E_2}$ by using plate characteristic functions and Timoshenko beam functions with $p = q = 8$ in equations (17) are shown in Table 2. For comparison, results obtained by the Rayleigh–Ritz solutions with characteristic polynomials [5] with $p = q = 5$ in equations (18), by the spline Rayleigh–Ritz method

TABLE 1

The frequency parameters, $\omega\sqrt{\rho a^2/E_2}$, of a five-layer orthotropic cross-ply laminated square plate ($0°/90°/0°/90°/0°$): $h/a = 0{\cdot}1$

(a) SSSS

Method			Mode 1	2	3	4	5
Iterative Kantorovich method	Number of iterations†	1	1·4218	2·7960	3·4843	4·2561	4·6179
		2	1·4202	2·7954	3·4830	4·2555	4·6163
Rayleigh–Ritz method‡	Using beam functions [4]		1·4204	2·7954	3·4832	4·2560	4·6166
	Using polynomials [5]		1·4207	2·8039	3·4956	4·2713	4·6409

(b) CCCC

Method			Mode 1	2	3	4	5
Iterative Kantorovich method	Number of iterations†	1	2·2442	3·3820	3·9395	4·7016	4·9765
		2	2·2217	3·3818	3·9294	4·7012	4·9761
Rayleigh–Ritz method‡	Using beam functions [4]		2·2216	3·3823	3·9297	4·7021	4·9764
	Using polynomials [5]		2·2226	3·3923	3·9416	4·7202	4·9943

† The relative error convergence criterion is 1×10^{-6}.

‡ Using beam functions and polynomials up to the fifth order in each direction.

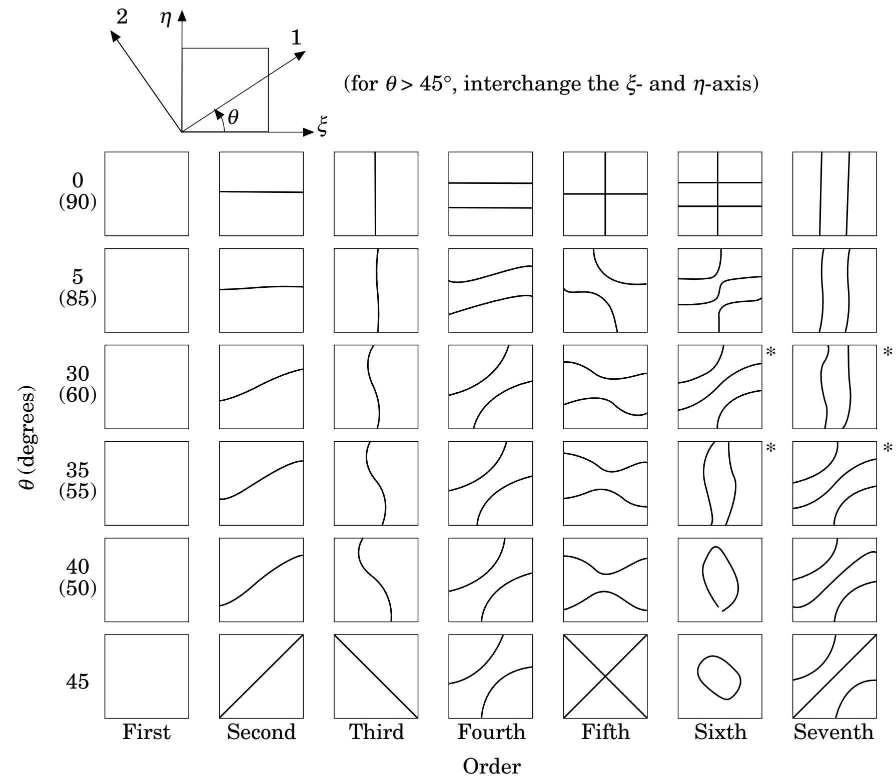

Figure 3. The nodal line patterns of an anisotropic single layer plate: CCCC, $h/a = 0{\cdot}1$. For the patterns marked with an asterisk, refer to Figure 4.

with the B_{32} spline functions [8] and by the spline finite strip method with eight spline sections [9] are shown together in this table. In Table 2 good agreement is shown between the results obtained by each method, but the results based on the class of Timoshenko

TABLE 2

The frequency parameters, $\omega\sqrt{\rho a^2/E_2}$, *of an anisotropic single layer square plate*: CCCC, $h/a = 0{\cdot}1$

	Rayleigh–Ritz method				
Mode	Using plate characteristic functions†	Using beam functions†	Using polynomials [5]‡	Using spline functions [8]§	Spline finite strip method [9]¶
1	1·2836	1·2935	1·3094	1·2774	1·2774
2	2·0080	1·9823	2·0057	1·9688	1·9679
3	2·4302	2·4579	2·4417	2·4026	2·4026
4	2·8357	2·8274	2·8286	2·8070	2·8051
5	3·1930	3·1867	—	—	—
6	3·6960	3·6937	—	—	—

† Using plate functions and beam functions up to the eighth order in each direction.
‡ Using polynomials up to the fifth order in each direction.
§ Six spline sections within a plate in each of the x and y directions.
¶ Eight spline sections within a plate.

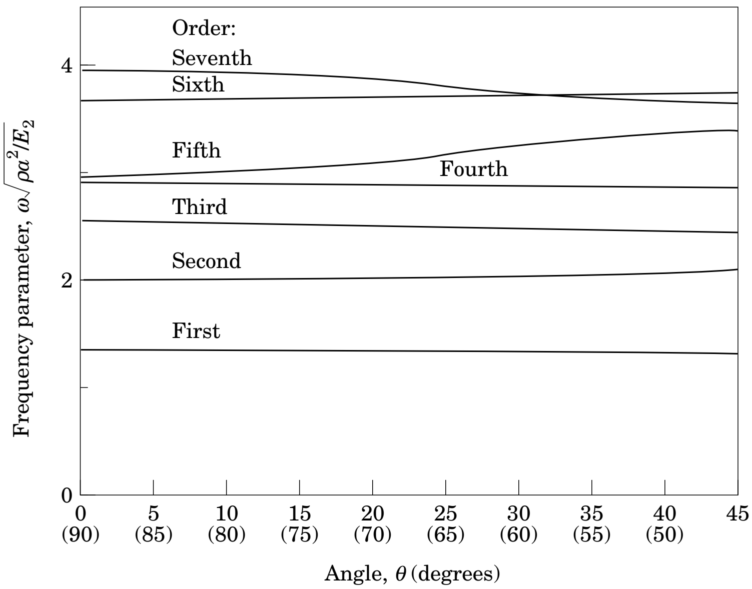

Figure 4. The frequency parameters, $\omega\sqrt{\rho a^2/E_2}$, versus the lamina orientation angle of an anisotropic single layer plate: CCCC, $h/a = 0{\cdot}1$.

beam functions (in columns 2, 3 and 4 of Table 2) are somewhat higher than those based on the spline functions due to overconstraint at the edges of the anisotropic plate.

In Figure 3 are also shown variations of nodal line patterns with respect to variations of the lamina orientation angle, θ. As shown in Figure 3, nodal line patterns of anisotropic angle-ply laminates are very complicated, but are systematic with respect to variations of the lamina orientation angle. It is also shown that nodal line patterns of the sixth and the seventh modes are interchanged at about $\theta = 32^\circ$ because the frequency parameters of these modes have very close values for $\theta = 30$–35°, as shown in Figure 4.

In Figure 5 are shown the calculated frequency parameters of two plate models with all edges equally restrained against rotation. As shown in Figure 5, the frequency parameters of higher modes are less dependent on the rotational restraint condition than those of lower modes. It is also shown that variations of the calculated frequencies due to changes in the restraint parameter are relatively larger in the orthotropic plate than in the anisotropic plate for the lower values of the restraint parameter. Also, edges having rotational restraint parameter values of over 1000 for the orthotropic plate and over 100 000 for the anisotropic plate can be regarded as clamped.

5.2. EXPERIMENTAL APPLICATIONS

Two marine woven roving laminated rectangular plates used in real structures of FRP ships, such as minesweepers, are adopted in experimental applications. The plates are made of 22 and 54 plies of E-glass woven roving with a weight density of 860 g/m^2 in isophthalic polyester resin by hand lay-up. The side lengths of two specimens are 1·8 m × 1·2 m. The thickness of the first specimen (specimen 1) is 24 mm, and that of the second specimen (specimen 2) is 51 mm. The warp and fill directions of woven roving of all plies are coincident with the plate co-ordinates. Two specimens have the same material properties given as follows: $E_w = 13{\cdot}72$ kN/mm^2, $E_f = 13{\cdot}03$ kN/mm^2, $G_{wf} = 3{\cdot}43$ kN/mm^2 and $\nu_{wf} = 0{\cdot}13$, where the subscripts w and f denote the warp and fill directions of woven roving.

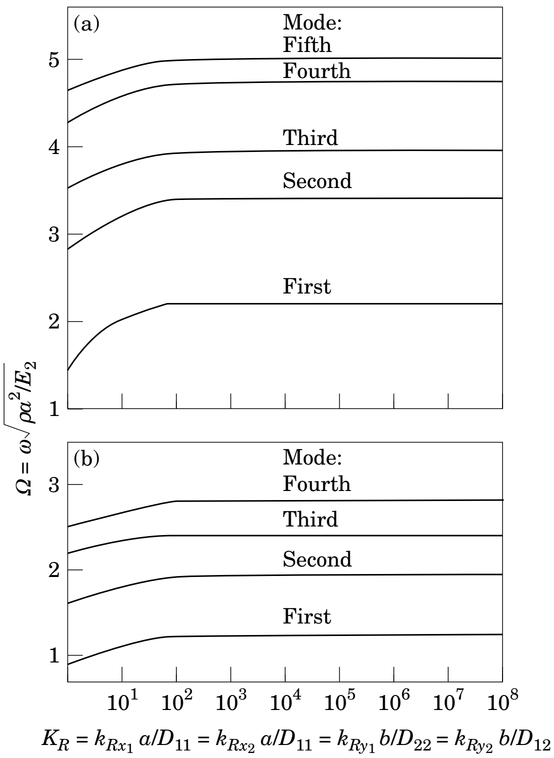

Figure 5. The frequency parameters, $\omega\sqrt{\rho a^2/E_2}$, versus the degree of elastic restraint against rotation along the boundary: $h/a = 0{\cdot}1$. (a) An orthotropic cross-ply plate; (b) an anisotropic single layer plate.

Experiments are performed for the boundary conditions of all edges clamped. Natural frequencies are determined by using an impact hammer test and a zoom-FFT analyzer, and modal damping values are identified by the half-power bandwidth method [16].

Table 3

Comparisons of the calculated natural frequencies and experimental values (*in* Hz) *for the marine woven roving laminated plates*: CCCC

	Specimen 1 (1800 mm × 1200 mm × 24 mm)			Specimen 2 (1800 mm × 1200 mm × 51 mm)		
	Calculation			Calculation		
Mode	Iterative Kantorovich method†	Rayleigh–Ritz by using polynomials‡	Experiment	Iterative Kantorovich method†	Rayleigh–Ritz by using polynomials‡	Experiment
1	59·5	59·5	54·8 (2·00)§	124·7	124·6	122·8 (4·37)
2	90·9	90·9	88·4 (1·09)	189·5	189·4	194·4 (1·35)
3	146·5	146·5	140·6 (1·33)	301·5	301·6	—
4	146·7	146·8	145·2 (0·91)	303·0	303·2	309·6 (0·87)
5	171·5	171·5	166·0 (0·74)	352·1	352·2	348·4 (1·62)
6	218·6	218·6	212·8 (0·81)	446·2	446·3	453·2 (0·75)

† The relative error convergence criterion is 1×10^{-6}.
‡ Using polynomials up to the eighth order in each direction.
§ The values in parentheses are modal damping ratio (%).

In Table 3 are shown experimental results of two specimens. For comparison, numerical results obtained by the iterative Kantorovich method and the Rayleigh–Ritz method using characteristic polynomials with $p = q = 8$ in equations (17) are shown together in the table. It is shown in Table 3 that the numerical results are in good agreement with each other as well as with the experimental ones.

6. CONCLUSIONS

Free vibration analysis of symmetrically laminated composite rectangular plates with all edges elastically restrained against rotation was carried out based on the YNS theory. The iterative Kantorovich method and the Rayleigh–Ritz method were applied to the vibration analysis. Three different sets of trial function, the newly derived plate characteristic functions, Timoshenko beam functions and characteristic polynomials, were used to obtain the Rayleigh–Ritz solution. The numerical results obtained by each method are compared with each other and with the experimental ones, and they showed good agreement. It is shown that the application of the iterative Kantorovich method to the vibration analysis of orthotropic cross-ply laminates is more effective in accuracy and efficiency than Rayleigh–Ritz analysis by using the aforementioned sets of trial functions, but is impractical to apply the iterative Kantorovich method to the vibration analysis of anisotropic angle-ply laminates directly because of skew nodal line patterns of anisotropic angle-ply laminates. In these cases, the Rayleigh–Ritz method using the derived plate characteristic functions is applicable to the analysis.

REFERENCES

1. P. C. Yang, C. H. Norris and Y. Stavsky 1966 *International Journal of Solids and Structures* **2**, 665–684. Elastic wave propagation in heterogeneous plates.
2. J. M. Whitney and N. J. Pagano 1966 *Transactions of the American Society of Mechanical Engineers*, *Journal of Applied Mechanics* **37**, 1031–1036. Shear deformation in heterogeneous anisotropic plates.
3. C. W. Bert and T. L. C. Chen 1978 *Computers and Structures* **14**, 465–473. Effect of shear deformation on vibration of antisymmetric angle-ply laminated rectangular plates.
4. T. J. Craig and D. J. Dawe 1986 *International Journal of Solids and Structures* **22**, 155–169. Flexural vibration of symmetrically laminated composite rectangular plates including shear effects.
5. T. Y. Chung and J. H. Chung 1992 *Transactions of the Society of Naval Architects of Korea* **29**, 140–148. Vibration analysis of symmetrically laminated composite rectangular plates (in Korean).
6. J. H. Chung, T. Y. Chung and K. C. Kim 1993 *Journal of Sound and Vibration* **163**, 151–163. Vibration analysis of orthotropic Mindlin plates with edges elastically restrained against rotation.
7. J. A. Bowlus, A. N. Palazotto and J. M. Whitney 1987 *International Journal of Solids and Structures* **22**, 155–169. Vibration of symmetrically laminated rectangular plates considering deformation and rotary inertia.
8. D. J. Dawe and S. Wang 1993 *Composite Structures* **25**, 77–87. Free vibration of generally-laminated, shear-deformable, composite rectangular plates using a spline Rayleigh–Ritz method.
9. D. J. Dawe and S. Wang 1995 *International Journal of Mechanical Science* **37**, 645–667. Spline finite strip analysis of the buckling and vibration of rectangular composite laminated plates.
10. R. B. Bhat, J. Singh and G. Mundkur 1993 *Transactions of the American Society of Mechanical Engineers*, *Journal of Vibration and Acoustics* **115**, 177–181. Plate characteristic functions and natural frequencies of vibration of plates by iterative reduction of partial differential equation.
11. J. M. Lee and K. C. Kim 1995 *Journal of Sound and Vibration* **187**, 865–877. Vibration analysis of rectangular thick plates using Mindlin plate characteristic functions.

12. T. S. Chia 1980 *Nonlinear Analysis of Plates*. New York: McGraw-Hill.
13. T. S. Chow 1971 *Journal of Composite Materials* **5**, 306–319. On the propagation of flexural waves in an orthotropic laminated plate and its response to an impulsive load.
14. J. M. Whitney 1973 *Transactions of the American Society of Mechanical Engineers*, *Journal of Applied Mechanics* **40**, 302–304. Shear correction factors for orthotropic laminates under static load.
15. D. J. Dawe and O. L. Roufaeil 1980 *Journal of Sound and Vibration* **69**, 345–359. Rayleigh–Ritz vibration analysis of Mindlin plates.
16. D. J. Ewins 1984 *Modal Testing*: *Theory and Practice*. Letchworth, Herts, U.K.: Research Studies Press.

APPENDIX

In this appendix, an exact method to obtain the solution of the boundary value problem as given in equations (11), (12) and (13) is presented.

The coupled differential equations (11) can be expressed in terms of the differential operator $\hat{D}$ $(=\mathrm{d}/\mathrm{d}\xi)$ as follows:

$$(\hat{D}^2 + \beta_{11}\hat{D} + \beta_{12})\Phi + (\gamma_{11}\hat{D}^2 + \gamma_{12}D + \gamma_{13})\frac{1}{a}X = 0,$$

$$(\gamma_{21}\hat{D}^2 + \gamma_{22}\hat{D} + \gamma_{23})\Phi + (\hat{D}^2 + \beta_{21}\hat{D} + \beta_{22})\frac{1}{a}X = 0. \tag{A1}$$

Eliminating Φ from equations (A1), the single differential equation with respect to X can be obtained as follows:

$$(\hat{D}^4 + A\hat{D}^3 + B\hat{D}^2 + C\hat{D} + E)\frac{1}{a}X = 0, \tag{A2}$$

where

$$A = (\gamma_{12}\gamma_{22} + \gamma_{12}\gamma_{21} - \beta_{21} - \beta_{11})(\gamma_{11}\gamma_{21} - 1)^{-1},$$

$$B = (\gamma_{11}\gamma_{23} + \gamma_{12}\gamma_{22} + \gamma_{13}\gamma_{21} - \beta_{12} - \beta_{11}\beta_{21} - \beta_{22})(\gamma_{11}\gamma_{21} - 1)^{-1},$$

$$C = (\gamma_{12}\gamma_{23} + \gamma_{13}\gamma_{22} - \beta_{11}\beta_{22} - \beta_{12}\beta_{21})(\gamma_{11}\gamma_{21} - 1)^{-1},$$

$$E = (\gamma_{13}\gamma_{23} - \beta_{12}\beta_{22})(\gamma_{11}\gamma_{21} - 1)^{-1}. \tag{A3}$$

Let m_i, $i = 1, 2, 3, 4$, be the solutions of the following auxiliary equation of (A2):

$$(\hat{D}^4 + A\hat{D}^3 + B\hat{D}^2 + C\hat{D} + E) = 0. \tag{A4}$$

Then, equation (A2) turns out to be

$$(\hat{D} - m_1)(\hat{D} - m_2)(\hat{D} - m_3)(\hat{D} - m_4)\frac{1}{a}X = 0, \tag{A5}$$

and the general solution of equation (A2) is as follows:

$$\frac{1}{a}X = c_1\,\mathrm{e}^{m_1\xi} + c_2\,\mathrm{e}^{m_2\xi} + c_3\,\mathrm{e}^{m_3\xi} + c_4\,\mathrm{e}^{m_4\xi}. \tag{A6}$$

Similarly, Φ can be obtained as follows:

$$\Phi = d_1\,\mathrm{e}^{m_1\xi} + d_2\,\mathrm{e}^{m_2\xi} + d_3\,\mathrm{e}^{m_3\xi} + d_4\,\mathrm{e}^{m_4\xi}. \tag{A7}$$

In equations (A6) and (A7), c_i and d_i ($i = 1, \ldots, 4$) are arbitrary constants. By substituting equations (A6) and (A7) into equations (A1), the relations between c_i and d_i are given, as follows:

$$d_i = -\frac{\gamma_{11} m_i^2 + \gamma_{12} m_i + \gamma_{13}}{m_i^2 + \beta_{11} m_i + \beta_{12}} c_i, \qquad i = 1, 2, 3, 4. \tag{A8}$$

From the general solutions (A6) and (A7), and the boundary conditions (12) and (13), an eigenvalue problem can be formulated in the following matrix form:

$$[\tilde{D}_{ij}]\{c_i\} = \{0\}, \qquad i, j = 1, 2, 3, 4, \tag{A9}$$

where

$$\tilde{D}_{1j} = \alpha \frac{D_{16}}{D_{11}} A_4 m_i + \alpha^2 \frac{D_{12}}{D_{11}} A_2 - \left(\frac{\gamma_{11} m_i^2 + \gamma_{12} m_i + \gamma_{13}}{m_i^2 + \beta_{11} m_i + \beta_{12}}\right)\left(m_i + \alpha \frac{D_{16}}{D_{11}} A_6 - K_{Rx_1}\right),$$

$$\tilde{D}_{2j} = m_i + \left(\alpha \frac{D_{26}}{D_{66}} B_7 - ab \frac{A_{45}}{D_{66}} B_9 + ab \frac{A_{45}}{D_{66}} B_8\right)$$

$$- \left(\frac{\gamma_{11} m_i^2 + \gamma_{12} m_i + \gamma_{13}}{m_i^2 + \beta_{11} m_i + \beta_{12}}\right)\left(\frac{1}{\alpha} \frac{D_{16}}{D_{66}} B_9 + B_4 - b^2 \frac{A_{55}}{D_{66}} B_2\right),$$

$$\tilde{D}_{3j} = \left[\alpha \frac{D_{16}}{D_{11}} A_4 m_i + \alpha^2 \frac{D_{12}}{D_{11}} A_2 - \left(\frac{\gamma_{11} m_i^2 + \gamma_{12} m_i + \gamma_{13}}{m_i^2 + \beta_{11} m_i + \beta_{12}}\right)\left(m_i + \alpha \frac{D_{16}}{D_{11}} A_6 + K_{Rx_2}\right)\right] \mathrm{e}^{m_i},$$

$$\tilde{D}_{4j} = \left[m_i + \left(\alpha \frac{D_{26}}{D_{66}} B_7 - ab \frac{A_{45}}{D_{66}} B_9 + ab \frac{A_{45}}{D_{66}} B_8\right)\right.$$

$$\left. - \left(\frac{\gamma_{11} m_i^2 + \gamma_{12} m_i + \gamma_{13}}{m_i^2 + \beta_{11} m_i + \beta_{12}}\right)\left(\frac{1}{\alpha} \frac{D_{16}}{D_{66}} B_9 + B_4 - b^2 \frac{A_{55}}{D_{66}} B_2\right)\right] \mathrm{e}^{m_i}, \qquad j = 1, \ldots, 4. \tag{A10}$$

The solution of equation (A9) gives the frequency parameter Ω_{ij} and the corresponding functions $X(\xi)$ and $\Phi(\xi)$.